Epitaxial evolution on buried cracks in a strain-controlled AlN/GaN superlattice interlayer between AlGaN/GaN multiple quantum wells and a GaN template*

Huang Cheng-Cheng(黄呈橙)[a], Zhang Xia(张 霞)[a], Xu Fu-Jun(许福军)[a)†], Xu Zheng-Yu(许正昱)[a], Chen Guang(陈 广)[a], Yang Zhi-Jian(杨志坚)[a], Tang Ning(唐 宁)[a], Wang Xin-Qiang(王新强)[a)b)], and Shen Bo(沈 波)[a)b)‡]

[a)] *State Key Laboratory of Artificial Microstructure and Mesoscopic Physics, School of Physics, Peking University, Beijing* 100871, *China*
[b)] *Collaborative Innovation Center of Quantum Matter, Beijing* 100871, *China*

(Received 28 April 2014; revised manuscript received 4 June 2014; published online 20 August 2014)

Epitaxial evolution of buried cracks in a strain-controlled AlN/GaN superlattice interlayer (IL) grown on GaN template, resulting in crack-free AlGaN/GaN multiple quantum wells (MQW), was investigated. The processes of filling the buried cracks include crack formation in the IL, coalescence from both side walls of the crack, build-up of an MQW-layer hump above the cracks, lateral expansion and merging with the surrounding MQW, and two-dimensional step flow growth. It was confirmed that the filling content in the buried cracks is pure GaN, originating from the deposition of the GaN thin layer directly after the IL. Migration of Ga adatoms into the cracks plays a key role in the filling the buried cracks.

Keywords: AlGaN/GaN, multiple quantum wells, epitaxial evolution

PACS: 61.66.Dk, 61.72.–y, 61.72.J–, 61.72.jd **DOI:** 10.1088/1674-1056/23/10/106106

1. Introduction

Recently, many groups have focused on GaN-based intersubband transition (ISBT) devices for infrared detection based on $Al_xGa_{1-x}N$/GaN (AlGaN/GaN) multiple quantum wells (MQW). AlGaN/GaN MQW structures offer significant potential for ISBT due to a large offset in the conduction band, enabling much wider spectrum detection and a very short relaxation time, enabling ultrafast optics devices.[1–5] When fabricating AlGaN/GaN MQW on GaN templates, cracking caused by tensile strain due to the large lattice mismatch is always an obstacle and a major problem.[6]

In our previous publication, we reported a strain control technique employing an AlN/GaN superlattice (SL) interlayer (IL).[7] It was found that the IL acts as a strain relief channel and works against cracking in the AlGaN/GaN MQWs. Cracks are generated in the IL, and then misfit dislocations form and relax the strain. The cracks in the IL are filled up immediately and then buried by the subsequent epilayer. Crack-free MQW are then grown on top of the IL. However, the mechanism and growth kinetics of buried crack formation and filling up processes remained unknown. In the present study, the growth evolution of the buried cracks has been investigated *ex-situ*, and the growth kinetics are discussed here in detail.

2. Experiments

The samples used in this study were grown on *c*-plane sapphire substrates by low pressure metal–organic chemical vapor deposition (MOCVD). Trimethylgallium, trimethylaluminum, and ammonia were used as Ga, Al, and N sources. First, a 2-μm-thick GaN template was grown under H_2 atmosphere at 1040 °C. After that, an IL consisting of 15 periods of 2-nm-AlN/1 nm-GaN SLs with the equivalent Al composition 0.66 was deposited at 1060 °C and then covered by a 20-nm-thick GaN layer to make the surface flat enough for deposition of the MQWs. Subsequently, 40 periods of $Al_{0.35}Ga_{0.65}N$/GaN MQWs were deposited. The barrier and well thickness were set to be 5 nm and 3 nm, respectively. Finally, the MQWs were covered by a 20-nm-thick $Al_{0.6}Ga_{0.4}N$ cap layer. The growth of the structures was interrupted several times to obtain samples for the growth evolution study. The structure is illustrated in Fig. 1.

After the growth, Seiko SPI-400 atomic force microscopy (AFM) and Tecnai F30 high-resolution transmission electron microscopy (HR-TEM) were used to characterize and investigate the surface morphologies and cross-sectional details. In addition, high-angle annular dark field scanning transmission electron microscopy (HAADF-STEM), combined with energy-dispersive X-ray spectroscopy (EDX), was applied to investigate the interfaces and compositional variation.

*Project supported by the National Natural Science Foundation of China (Grant Nos. 11174008 and 61361166007), the National Basic Research Program of China (Grant Nos. 2012CB619306 and 2012CB619301), and the Research Fund for the Doctoral Program of Higher Education of China (Grant No. 20100001120012).

†Corresponding author. E-mail: fjxu@pku.edu.cn
‡Corresponding author. E-mail: bshen@pku.edu.cn

© 2014 Chinese Physical Society and IOP Publishing Ltd

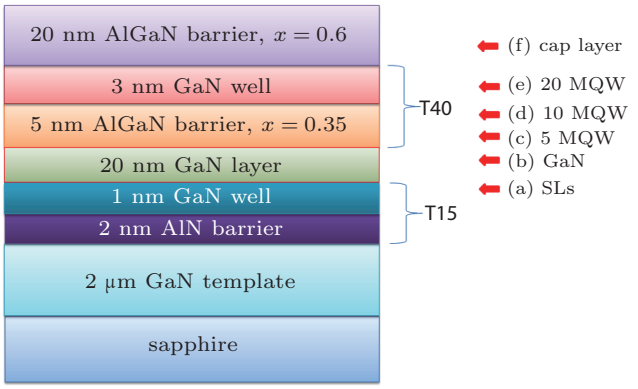


Fig. 1. (color online) Schematic structure of AlGaN/GaN MQW grown on AlN/GaN SL interlayer. The arrows indicate the growth interruption at different stages.

3. Results and discussion

To study the growth evolution of the cracks generated in the IL and the filling-up processes during the subsequent epitaxial growth, the surface morphology was *ex-situ* characterized at each stage by AFM. A typical surface morphology after deposition of the SL IL is shown in Fig. 2(a). A crack in the surface is clearly shown lying along the $\langle 11\bar{2}0\rangle$ direction, suggesting that cracks are indeed generated during growth of the SL IL. Figure 2(b) shows the surface morphology after deposition of the thin GaN layer on top of the SL IL. Some parts of the crack tend to merge together from both side walls. Figure 2(c) shows the surface morphology after deposition of five periods of MQW. The crack has already coalesced and the MQW layer located above the buried crack is found to be higher than the surrounding area, which indicates that the growth rate above the buried crack exceeds that of the areas farther from cracks. The coalescence of both side walls of the crack finally leads to an MQW-layer hump above the buried crack. The hump is several nm high with a span of about 200 nm. Figures 2(d) and 2(e) show the surface morphology after 10 and 20 periods of MQW deposition, respectively. The hump continues to expand laterally and gradually merges with the surrounding parts of the MQW layer. Meanwhile, a step flow mode is conducted and clear atomic steps develop. Figure 2(f) shows the surface morphology of the entire structure after deposition of 40 periods of MQW and the cap layer.

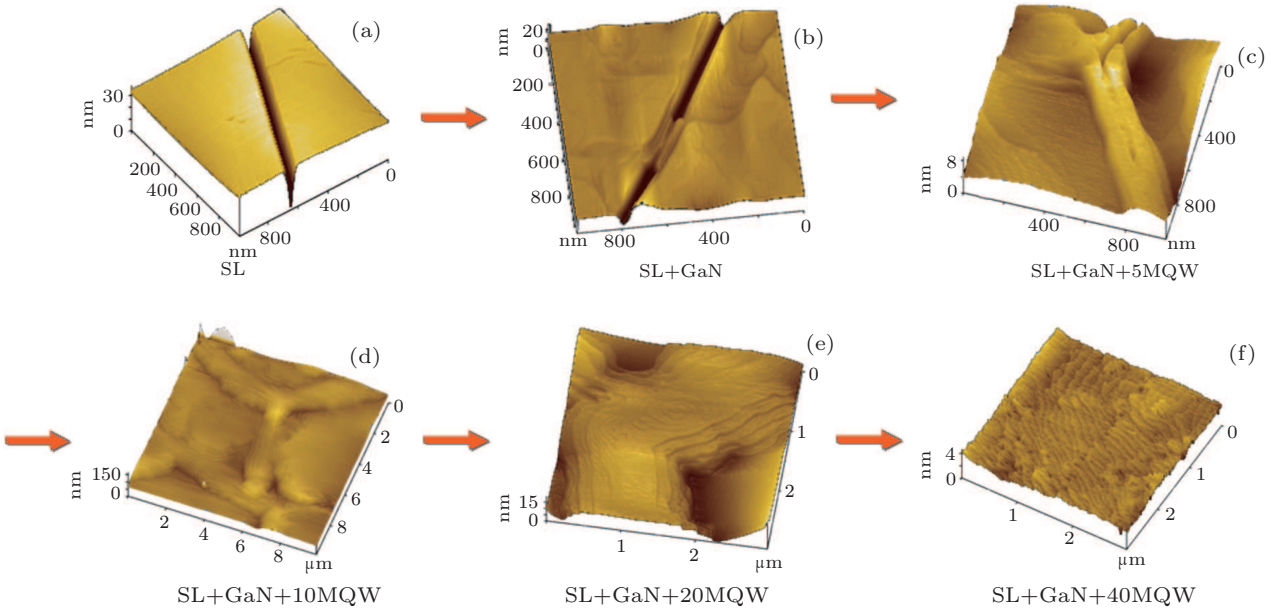


Fig. 2. (color online) Surface morphology at different growth stages.

To further examine the filling up process around the buried cracks, cross sectional TEM was employed. Figure 3(a) shows the cross sectional *Z*-contrast image from the HAADF-STEM, taken along the $\langle 10\bar{1}0\rangle$ zone axis. The GaN template, SL IL, and the MQW layer are distinguished separately by *Z*-contrast. It is clear that a trapezoid region with light contrast on a 50-nm scale is located in the dark contrast SL IL. The trapezoidal region gives evidence of the existence of a crack (vertical cross section) in the SL IL. The trapezoidal region could be more precisely described as a V-shaped region, because the apex of the V shape extends into the GaN template. In addition, no void is found in this V-shaped region, suggesting that the buried crack has been totally filled up during the subsequent epitaxial layer.

Figure 3(b) shows the details around the V-shaped region under higher magnification, by HAADF-STEM. Two sets of fringes correspond to the short-period SL IL (darker), and the long-period MQW (lighter). Note that the *Z* contrast in the V-shaped region is similar to the one in the GaN template, which differs from the periodic dark and light contrast variation in the

SL IL. This fact implies that the composition in the V-shaped region is uniform. Besides, it can be observed that the interfaces of the first few quantum wells above the buried crack are slightly bent outward, and the well and barrier thicknesses are not uniform. The appearance of bent MQW is consistent with the hump of MQW above the buried crack shown in Fig. 2. The degree of bending shrinks, and it vanishes after 10 periods of MQW deposition, by which time the interfaces become straight and sharp, and the well and barrier become uniform.

EDX line scans were taken to determine the composition in the region. Line 1 in Fig. 4(a) shows a 80-nm-long scan line which vertically crosses through the SL IL from the GaN template into the MQW layer. Line 2 is an equally long scan line which vertically crosses through the V-shaped region. The signals of Ga and Al elements in Lines 1 and 2 are extracted and plotted in Fig. 4(b). The scan electron spot is focused on the GaN template layer at the beginning in Line 1, so only the Ga signal is present. As the spot moves into the SL IL, the Ga signal decreases while the Al signal increases. When the spot moves into the MQW layer, where the average Al composition is lower than that in the SL IL, the signals of Ga and Al elements reverse their trends.

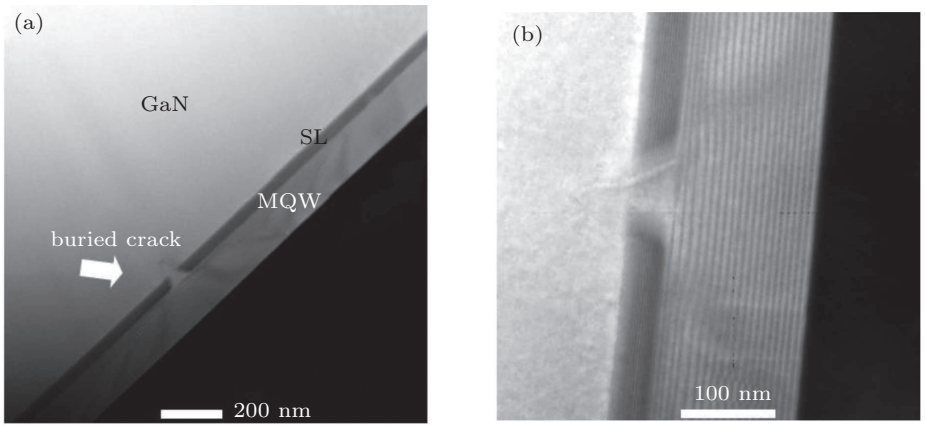


Fig. 3. HAADF-STEM images of cross-sectional sample under (a) low magnification and (b) high magnification.

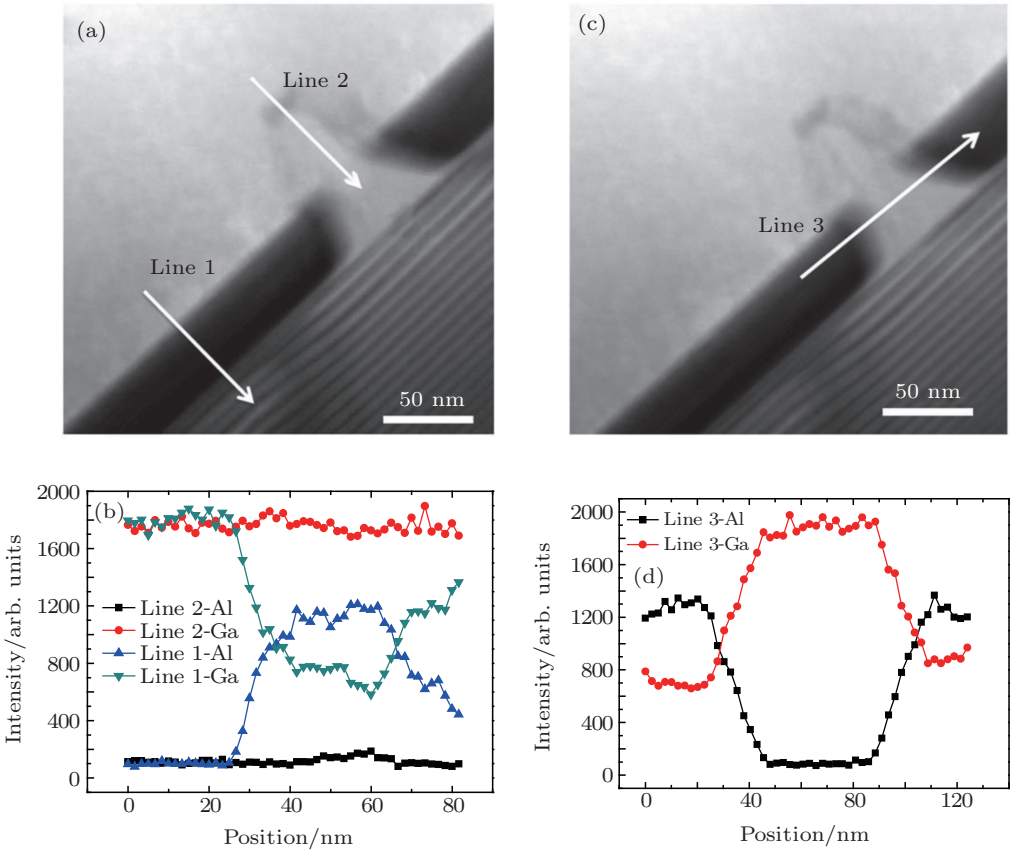


Fig. 4. (color online) (a) Two parallel scan lines of EDX that cross through the SL IL and V-shaped region vertically. (b) Signals of Ga and Al elements in scanned Lines 1 and 2. (c) Scan line of EDX which cross through the V-shaped region horizontally. (d) Signals of Ga and Al elements in scanned Line 3.

Unlike in Line 1, in Line 2 the Ga signal is almost constant at a high level, while the Al signal is absent during the whole scan. Line 3, shown in Fig. 4(c), is another scan line crossing the V-shaped region horizontally. When the scan electron spot is in the SL IL, the signals of Ga and Al are around 800 and 1200, respectively. When the spot moves into the V-shaped region, the Ga signal goes up to about 1800, while the Al signal drops to around zero. These EDX results, shown by Lines 2 and 3, demonstrate that the main filling content in the V-shaped region (i.e. the buried crack) is pure GaN.

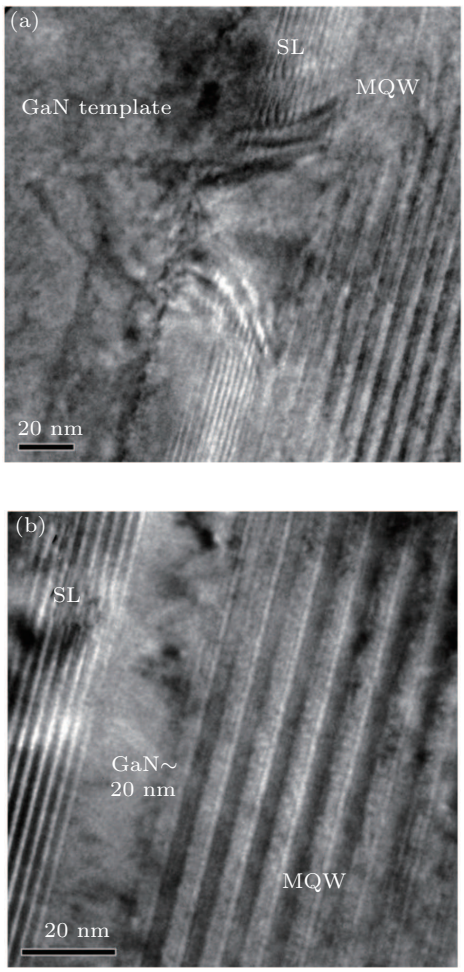


Fig. 5. Cross-sectional HR-TEM observations taken (a) near and (b) far from a buried crack.

To confirm the origin and process of GaN filling up the buried cracks, more cross-sectional HR-TEM observations were made, both near and far away from a buried crack in the SL IL. Figure 5(a) shows the image near a buried crack. The MQW layer is directly on top of the SL IL, and is not separated by the GaN thin layer. Figure 5(b) shows a contrasting image of a joint part of MQW and SL that is located far from the buried cracks. It is clear that the 20-nm-thick GaN layer is sandwiched between the SL and the MQW layers. Therefore, the absence of the thin GaN layer near the buried cracks implies that adatoms move about in this region during growth. When the cracks are generated in the SL IL, Ga adatoms on the surface are diffusing and tend to settle into the cracks. This significantly depletes the Ga adatoms within a certain distance from the cracks. We determined the distance within which the GaN thin layer is depleted by HADDF-STEM. It was found that with increasing distance from the buried crack, the GaN thin layer gradually becomes thicker. At a distance of 1 μm∼2 μm, the thickness of GaN thin layer recovers to around 20 nm. This distance can be regarded as the diffusion length of Ga adatoms in this system. In addition, the side wall facet of the buried cracks can also be determined from Fig. 5(a) since it is taken precisely along the $\langle 10\bar{1}0\rangle$ zone axis. The angle between the inclined side wall facet and the *c* plane is about 70°, thus the side walls of the buried crack correspond to the $\{10\bar{1}1\}$ crystal planes.

Based on the above results, the growth evolution kinetics of buried cracks is illustrated in Fig. 6. To simplify our model, we mainly focus on the surface process of Ga adatoms, without giving regard to the chemical reactions on the surface.[8–10] Figure 6(a) shows the evolution onset with a 2-μm-thick GaN template with an atomically smooth surface. Then, the AlN/GaN SL IL is grown on the template with the equivalent Al composition 0.66 and the thickness of 50 nm. Tensile strain, which is due to the great lattice mismatch between the GaN template and the SL IL, leads to cracking along the $\langle 11\bar{2}0\rangle$ direction. The crack has a V-shaped cross section with the apex extending into the GaN template, as shown in Fig. 6(b). The side wall facet is the $\{10\bar{1}1\}$ crystal plane, which consists of many steps at atomic scale, as shown in Fig. 6(c). These atomic steps can act as nucleation sites for Ga adatom absorption and incorporation into the lattice. When a Ga adatom meets a V-shaped crack during the diffusion process, it will continue to migrate onto the inclined $\{10\bar{1}1\}$ face because the face has greater surface energy than the (0001) plane. This means that Ga adatoms tend to fill up the crack. Therefore, the growth competition between the [0001] direction and the direction perpendicular to the $\{10\bar{1}1\}$ faces should dominate the crack filling, which eventually fills the V-shaped cracks with GaN. Meanwhile, Ga adatoms within a certain distance from the crack are somewhat depleted. So a hump forms above the buried crack due to the fast growth on the crack and depletion of GaN in the surrounding area, as indicated by the dashed line in Fig. 6(d).

Figure 6(e) shows the surface process when the deposition of MQW continues after the crack has been filled. Due to the hump above the buried cracks, the first few periods of MQW deposition will conform to the surface shape, bending outward slightly, as proved by our STEM result in Fig. 3(b). Due to the depletion of GaN near the buried cracks, the thin GaN layer increases gradually in thickness with increasing distance from the buried cracks. Meanwhile, under optimal

growth conditions, the lateral growth of MQWs is enhanced and the hump expands and coalesces with the surrounding MQWs. This will finally lead to a coherent and smooth MQW layer, as illustrated in Fig. 6(f).

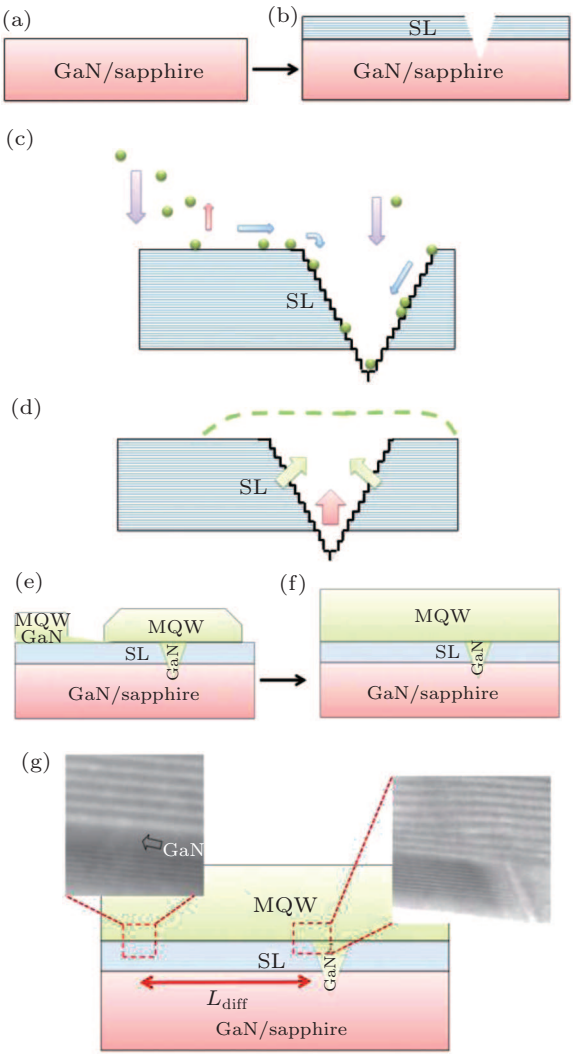


Fig. 6. (color online) Model of growth evolution kinetics illustrating the processes of filling the buried cracks.

Figure 6(g) illustrates the diffusion length of Ga adatoms. The distance is about 1∼2 μm according to our HAADF-STEM results, shown in the insets, which is on the same order as the result of 535 nm of Narita *et al.*[11] Generally, the diffusion length can be expressed as $L_{\rm diff} = \sqrt{D_{\rm s}\tau}$, where $D_{\rm s}$ is the diffusion coefficient and τ is the diffusion lifetime. The diffusion coefficient can be expressed as $D_{\rm s} = \lambda^2 \nu_{\rm s} {\rm e}^{-E/kT}$, where λ is the hopping distance of an atom between two neighboring sites, $\nu_{\rm s}$ is the test frequency with a representative value of 10^{12}/s, E is the energy barrier of surface diffusion, k is the Boltzmann constant, and T is the temperature on the surface. The energy barrier for a Ga adatom on a (0001) Ga-polar GaN surface has been obtained by many groups employing density-functional theory.[12–14] For example, Takeuchi *et al.* got the value of $E = 0.63$ eV.[13] We chose the parameters $T = 1300$ K, $\lambda = 0.3189$ nm, and $L_{\rm diff} = 1$ μm–2 μm, as mentioned in our experiments. Thus, the diffusion lifetime of Ga adatoms is estimated to be $\tau = 2.6 \times 10^{-3}$ s–1×10^{-2} s based on the above model.

4. Conclusion

In conclusion, the growth evolution of buried cracks in strain-controlled AlN/GaN SL IL, resulting in crack-free AlGaN/GaN MQWs, has been investigated. The kinetic process was revealed by *ex-situ* atomic force microscopy, including crack formation in the IL, coalescence from both side walls of the crack, a hump above the buried cracks, lateral expansion and merging with the surrounding MQWs, and a two-dimensional step flow growth mode. It was also confirmed that the filling content in the buried cracks is pure GaN, which originates from the deposition of the GaN thin layer directly after the IL. Migration of Ga adatoms into the cracks plays a key role in filling the buried cracks. The diffusion length of Ga adatoms was measured to be 1 μm–2 μm, and the diffusion lifetime was estimated to be 2.6×10^{-3} s–1×10^{-2} s.

References

[1] Tchernycheva M, Nevou L, Doyennette L, Julien F H and Warde E 2006 *Phys. Rev. B* **73** 125347
[2] Driscoll K, Bhattacharyya A, Moustakas T D, Paiella R, Zhou L and Smith D J 2007 *Appl. Phys. Lett.* **91** 141104
[3] Kandaswamy P K, Guillot F, Monroy E, Nevou L, Tchernycheva M, Michon A, Julien F H, Baumann E, Giorgetta F R, Hofstetter D, Remmele T, Albrecht M, Birner S and Dang L S 2008 *J. Appl. Phys.* **104** 093501
[4] Yang J, Sodabanlu H, Sugiyama M and Nakano Y 2009 *Appl. Phys. Lett.* **95** 162111
[5] Hofstetter B D, Baumann E, Giorgetta F R, Wu H, Schaff W J, Ieee M, Dawlaty J, George P A, Eastman L F, Ieee F, Rana F, Kandaswamy P K, Guillot F and Monroy E 2010 *Proc. IEEE* **98** 1234
[6] Huang C C, Xu F J, Yan X D, Song J, Xu Z Y, Cen L B, Wang Y, Pan J H, Wang X Q, Yang Z J, Shen B, Zhang B S, Chen X S and Lu W 2011 *Appl. Phys. Lett.* **98** 132105
[7] Huang C C, Xu F J, Song J, Xu Z Y and Wang J M 2012 *J. Appl. Phys.* **111** 016105
[8] Thon A and Kuech T F 1996 *Appl. Phys. Lett.* **69** 55
[9] Sengupta D, Mazumder S and Kuykendall W 2005 *J. Cryst. Growth* **279** 369
[10] Mihopoulos T G, Gupta V and Jensen K F 1998 *J. Cryst. Growth* **195** 733
[11] Narita T, Hikosaka T, Honda Y and Yamaguchi M 2003 *Phys. Stat. Sol.* **0** 2154
[12] Jindal V, Shahedipour-sandvik F, Jindal V and Shahedipour-sandvik F 2010 *J. Appl. Phys.* **107** 054907
[13] Takeuchi N, Selloni A, Myers T H and Doolittle A 2005 *Phys. Rev. B* **72** 115307
[14] Zywietz T, Neugebauer J and Scheffler M 1998 *Appl. Phys. Lett.* **73** 487